Effect of centrality bin width corrections on two-particle number and transverse momentum differential correlation functions

Victor Gonzalez, Ana Marin, Pedro Ladron de Guevara, Jinjin Pan, Sumit Basu, and Claude A. Pruneau

Phys. Rev. C **99**, 034907 — Published 19 March 2019

DOI: 10.1103/PhysRevC.99.034907

Effect of centrality bin width corrections on two-particle number and transverse momentum differential correlation functions

Victor Gonzalez,[1,2,*] Ana Marin,[2] Pedro Ladron de Guevara,[1,3]
Jinjin Pan,[4,†] Sumit Basu,[4,‡] and Claude A. Pruneau[4]

[1] *Universidad Complutense de Madrid, Spain*
[2] *GSI Helmholtzzentrum für Schwerionenforschung, Research Division and ExtreMe Matter Institute EMMI, Darmstadt, Germany*
[3] *Instituto de Fisica, Universidad Nacional Autonoma de Mexico, Mexico City, Mexico*
[4] *Department of Physics and Astronomy, Wayne State University*

(Dated: December 16, 2018)

Two-particle number and transverse momentum differential correlation functions are powerful tools for unveiling the detailed dynamics and particle production mechanisms involved in relativistic heavy-ion collisions. Measurements of transverse momentum correlators P_2 and G_2, in particular, provide added information not readily accessible with better known number correlation functions R_2. However, it is found that the R_2 and G_2 correlators are somewhat sensitive to the details of the experimental procedure used to measure them. They exhibit, in particular, a dependence on the collision centrality bin-width, which may have a rather detrimental impact on their physical interpretation. A technique to correct these correlators for collision centrality bin-width averaging is presented. The technique is based on the hypothesis that the shape of single- and pair- probability densities vary slower with collision centrality than the corresponding integrated yields. The technique is tested with Pb–Pb simulations based on the HIJING and UrQMD models and shown to enable a precision better than 1% for particles in the kinematic range $0.2 \leq p_{\mathrm{T}} \leq 2.0$ GeV/c.

PACS numbers: 25.75.Gz, 25.75.Ld, 24.60.Ky, 24.60.-k

* victor.gonzalez@ucm.es
† jinjin.pan@cern.ch
‡ sumits.basu@cern.ch

I. INTRODUCTION

Measurements of correlation functions enable in-depth exploration of particle production mechanisms in relativistic heavy-ion collisions (HIC). Together with measurements of the nuclear modification factor, R_{AA}, measured number correlation functions have provided strong evidence for the formation of a dense and opaque medium, a Quark Gluon Plasma (QGP), in the midst of high energy heavy-ion collisions [1–9]. Measurements of transverse momentum differential correlation functions have also been added to the experimental toolset [10, 11]. For these as for differential number correlation functions, precision measurements require to account for a number of experimental conditions and artifacts [12]. In this paper, the sensitivity of two-particle differential correlators to the protocol used to account for centrality bin width averaging is studied, and correction techniques to account for finite collision centrality bins used in typical HIC analyses are considered.

Whether measuring two-particle number or transverse momentum differential correlation functions towards the study of collective behavior, the elucidation of particle production mechanisms, or the analysis of collision systems' evolution towards equilibrium, most data analyses are typically limited by the available statistics. Analyses are thus carried out with somewhat wide collision centrality bins and aim to report the evolution of the observables with centrality while accounting for the limited number of events. It is well established [1–9] that both the shape and strength of two-particle correlations evolve with collision centrality, i.e., the number, N_w, of nucleons wounded in a given collision. Normalized two-particle cumulant based correlators such as R_2, P_2, and G_2, defined below, scale as the inverse of the number of wounded N_w, or the number of nucleon participants, for collisions involving no collectivity and no rescattering of secondaries. Both the amplitude and the shape of these correlators thus indeed evolve with collision centrality. However, measurements of correlation functions are often carried out using fairly wide centrality bins amounting to 5%, 10%, or even larger values of the total interaction cross-section. Effectively, if events within a given centrality bin are analyzed indiscriminately, measured values of the correlator R_2, P_2, and G_2 will amount to some average across the width of the centrality bins. The issue arises, however, that such averages may not be properly calculated unless one explicitly accounts for the fact these three correlators are ratios of quantities that might behave differently across the bins. The mean value theorem, written

$$f(x_0) = \frac{\int_a^b f(x)dx}{b-a}, \tag{1}$$

stipulates that the mean value of a function across an interval $[a, b]$ is equal to the value of the function evaluated at x_0, a value of x within the interval $[a, b]$. In general x_0 does not correspond to the center of the bin. As will be shown, the correlator R_2 is a ratio of a two-particle density by the square (essentially) of a single particle density. Both the single- and pair-densities are functions of centrality. Evaluation of the average of these densities across a centrality bin involves integrals of the form given by Eq. (1). The two functions are evaluated across the same interval but may feature significantly different dependence on the centrality, i.e., variable x in Eq. (1). The two estimated densities end up corresponding to different values of x (centrality). The R_2 correlator, if evaluated as a ratio of these integrals, then amounts to a ratio of quantities evaluated at two distinct and unknown values of x. It is thus intrinsically biased and does not constitute a proper estimator of the average of R_2 across the centrality bin. A correction must thus be made to account for or suppress this bias. It will be shown that similar considerations also apply to the correlators P_2 and G_2. In addition to the width of the centrality bin, the magnitude of the corrections might also depend on the rate at which these correlators evolve with collision centrality. It is thus useful to invoke existing heavy-ion collision models to obtain quasi-realistic correlation functions and simulate their evolution with collision centrality. These can then be used to assess the magnitude of the corrections and systematic uncertainties associated with such corrections.

Correction procedures similar to those presented in this work were used in prior studies but were never formally published. The STAR collaboration used the correction procedure towards the study of differential two-particle transverse momentum correlations in Au–Au collisions [13], whereas the ALICE collaboration for measurements of the R_2 and P_2 correlators in p–Pb and Pb–Pb collisions [14]. This work establishes a formal record and documentation of these procedures and presents an estimate of their accuracy based on HIJING and UrQMD, two semi-realistic heavy-ion collisions models.

This letter is organized as follows. Inclusive and conditional particle densities are defined in sec. II. The impact of the Centrality bin width and a correction formula are first derived for normalized two-particle cumulants (two-particle number differential correlations) in sec. III. The study is then extended to momentum correlation functions in sec. IV. In sec. V, estimates of the precision of the method based on simulations carried out with the HIJING [15] and UrQMD [16, 17] particle event generators are presented. This work is summarized in sec. VI.

II. OBSERVABLE DEFINITIONS

Whether analyzing pp, p–Pb, or A–A collisions, it is legitimate to classify events on the basis of the energy, $E_{\rm ref}$, or the charged particle multiplicity, m, measured in a reference acceptance $\Omega_{\rm ref}$. Studies [18] have shown that in A–A collisions, this multiplicity maps rather narrowly onto the impact parameter b of the collisions, particularly in the case of mid- to central-collisions. While such narrow mapping does not exist for p–A or pp interactions, it remains appropriate to classify collisions based on the multiplicity m as it provides some measure of the momentum transfer and projectile kinetic energy dissipated in the collisions. In general, one indeed finds that the single and pair density measured in the fiducial acceptance $\Omega_{\rm ref}$ are functions of the reference multiplicity m. Thus single- and two-particle conditional densities (i.e., for a given m) are defined as

$$\rho_1(\eta,\varphi,p_{\rm T}|m) = \frac{1}{p_{\rm T}}\frac{dN}{d\varphi d\eta dp_{\rm T}}\bigg|_m \tag{2}$$

$$\rho_2(\eta_1,\varphi_1,p_{{\rm T},1},\eta_2,\varphi_2,p_{{\rm T},2}|m) = \frac{1}{p_{{\rm T},1}p_{{\rm T},2}}\frac{d^2N}{d\varphi_1 d\eta_1 dp_{{\rm T},1} d\varphi_2 d\eta_2 dp_{{\rm T},2}}\bigg|_m \tag{3}$$

Typically, correlation analyses are carried out over fixed $p_{\rm T}$ ranges $[p_{\rm T,min}, p_{\rm T,max}]$. One thus also defines conditional single- and two-particle densities integrated over $p_{\rm T}$ as

$$\rho_1(\eta,\varphi|m) = \int \rho_1(\eta,\varphi,p_{\rm T}|m)dp_{\rm T}, \tag{4}$$

$$\rho_2(\eta_1,\varphi_1,\eta_2,\varphi_2|m) = \int \rho_2(\eta_1,\varphi_1,p_{{\rm T},1},\eta_2,\varphi_2,p_{{\rm T},2}|m)dp_{{\rm T},1}dp_{{\rm T},2} \tag{5}$$

where (here and in the following) it is understood that the integrals in $p_{\rm T}$ are taken over the fixed range $[p_{\rm T,min}, p_{\rm T,max}]$. In practice, it is usually not possible (or meaningful) to measure the densities $\rho_1(\eta,\varphi|m)$ and $\rho_2(\eta_1,\varphi_1,\eta_2,\varphi_2|m)$ for unit resolution in m. One must then evaluate the densities within finite width bins of multiplicity $[m_{{\rm min},k}, m_{{\rm max},k}]$ (where $k = 1,\ldots,K$, represents one of K "centrality" bins used in the analysis) as weighted average of the densities across the bins according to

$$\bar{\rho}_1^{(k)}(\eta,\varphi) = \frac{1}{Q_k}\sum_{m=m_{{\rm min},k}}^{m_{{\rm max},k}} q(m)\rho_1(\eta,\varphi|m), \tag{6}$$

$$\bar{\rho}_2^{(k)}(\eta_1,\varphi_1,\eta_2,\varphi_2) = \frac{1}{Q_k}\sum_{m=m_{{\rm min},k}}^{m_{{\rm max},k}} q(m)\rho_2(\eta_1,\varphi_1,\eta_2,\varphi_2|m), \tag{7}$$

with

$$Q_k = \sum_{m=m_{{\rm min},k}}^{m_{{\rm max},k}} q(m) \tag{8}$$

and $q(m)$ representing the probability of events with multiplicity m in the reference acceptance.

III. NORMALIZED CUMULANTS: R_2

Two-particle normalized cumulants [12] are defined according to

$$R_2(\eta_1,\varphi_1,\eta_2,\varphi_2) = \frac{\rho_2(\eta_1,\varphi_1,\eta_2,\varphi_2) - \rho_1(\eta_1,\varphi_1)\rho_1(\eta_2,\varphi_2)}{\rho_1(\eta_1,\varphi_1)\rho_1(\eta_2,\varphi_2)} \tag{9}$$

and form the basis of many two-particle correlation analyses. For a recent study on the evolution with centrality of the two-particle differential number density correlation R_2 in p–Pb and Pb–Pb collisions, by the ALICE collaboration see Ref. [24]. Experimentally, in the study of A–A collisions, it is common to average R_2 across large collision centrality

bins. Given the width of such bins may depend on the specificities of a given experiment (e.g., the size of the reference acceptance), normalized cumulants R_2 are thus bin-width dependent. A correction procedure is then required to account for the finite width of the centrality bins.

In principle, one would like to set the collision centrality bins in terms of collision impact parameter ranges (alternatively the number of wounded nucleons). In practice, only proxies of the impact parameter are at best possible and one usually expresses the bins directly in terms of such proxies or in terms of the fractional cross-section measured within a centrality (multiplicity) bin. Let m, the multiplicity measured in the reference acceptance $\Omega_{\rm ref}$ represent such a proxy. As for densities, one can thus define conditional normalized cumulants according to

$$R_2(\eta_1,\varphi_1,\eta_2,\varphi_2|m) \;=\; \frac{\rho_2(\eta_1,\varphi_1,\eta_2,\varphi_2|m)}{\rho_1(\eta_1,\varphi_1|m)\rho_1(\eta_2,\varphi_2|m)} - 1. \tag{10}$$

However, measurements of $R_2(\eta_1,\varphi_1,\eta_2,\varphi_2|m)$ for m unit resolution are typically not possible due to limitations associated with the finite size of datasets, CPU time, or storage considerations. It is also impractical to report differential correlators $R_2(\eta_1,\varphi_1,\eta_2,\varphi_2|m)$ for a very large number of values of m. In practice, one thus seeks to report correlators R_2 averaged over reference multiplicity bins $[m_{\min,k}, m_{\max,k}]$. As for averages of densities defined in sec. II, this is nominally achieved according to

$$\bar{R}_2^{(k)}(\eta_1,\varphi_1,\eta_2,\varphi_2) \;=\; \frac{1}{Q_k}\sum_{m=m_{\min,k}}^{m_{\max,k}} q(m) R_2(\eta_1,\varphi_1,\eta_2,\varphi_2|m), \tag{11}$$

where $q(m)$ represents the probability of events with multiplicity m in the reference acceptance. One may then determine $R_2^{(k)}$ according to

$$R_2^{(\mathrm{Bin},k)}(\eta_1,\varphi_1,\eta_2,\varphi_2) \;=\; \frac{\rho_2^{(\mathrm{Bin},k)}(\eta_1,\varphi_1,\eta_2,\varphi_2)}{\rho_1^{(\mathrm{Bin},k)}(\eta_1,\varphi_1)\rho_1^{(\mathrm{Bin},k)}(\eta_2,\varphi_2)} - 1, \tag{12}$$

in which $\rho_1^{(\mathrm{Bin},k)}$ and $\rho_2^{(\mathrm{Bin},k)}$ are single- and pair-densities measured directly using finite width bins in m. In the absence of biases or event detection inefficiencies, one has

$$\rho_1^{(\mathrm{Bin},k)}(\eta_1,\varphi_1) \;=\; \bar{\rho}_1^{(k)}(\eta,\varphi), \tag{13}$$

$$\rho_2^{(\mathrm{Bin},k)}(\eta_1,\varphi_1,\eta_2,\varphi_2) \;=\; \bar{\rho}_2^{(k)}(\eta_1,\varphi_1,\eta_2,\varphi_2). \tag{14}$$

The quantities $R_2^{(\mathrm{Bin},k)}$ and $\bar{R}_2^{(k)}$ are thus clearly distinct:

$$R_2^{(\mathrm{Bin},k)}(\eta_1,\varphi_1,\eta_2,\varphi_2) \;=\; \frac{\frac{1}{Q_k}\sum_{m=m_{\min,k}}^{m_{\max,k}} q(m)\rho_2(\eta_1,\varphi_1,\eta_2,\varphi_2|m)}{\left[\frac{1}{Q_k}\sum_{m=m_{\min,k}}^{m_{\max,k}} q(m)\rho_1(\eta_1,\varphi_1|m)\right]\left[\frac{1}{Q_k}\sum_{m'=m_{\min,k}}^{m_{\max,k}} q(m')\rho_1(\eta_2,\varphi_2|m')\right]} - 1, \tag{15}$$

$$\bar{R}_2^{(k)}(\eta_1,\varphi_1,\eta_2,\varphi_2) \;=\; \left[\frac{1}{Q_k}\sum_{m=m_{\min,k}}^{m_{\max,k}} q(m)\frac{\rho_2(\eta_1,\varphi_1,\eta_2,\varphi_2|m)}{\rho_1(\eta_1,\varphi_1|m)\rho_1(\eta_2,\varphi_2|m)}\right] - 1. \tag{16}$$

To quantify the difference, the particle densities are written in terms of single- and two-particle probability densities, $\mathbb{P}_1(\eta,\varphi|m)$ and $\mathbb{P}_2(\eta_1,\varphi_1,\eta_2,\varphi_2|m)$ according to

$$\rho_1(\eta,\varphi|m) \;=\; \langle n\rangle_m \mathbb{P}_1(\eta,\varphi|m), \tag{17}$$

$$\rho_2(\eta_1,\varphi_1,\eta_2,\varphi_2|m) \;=\; \langle n(n-1)\rangle_m \mathbb{P}_2(\eta_1,\varphi_1,\eta_2,\varphi_2|m), \tag{18}$$

where, by definition, $\mathbb{P}_1$ and $\mathbb{P}_2$ respectively satisfy

$$\int d\varphi d\eta\, \mathbb{P}_1(\eta,\varphi|m) = 1 \tag{19}$$

$$\int d\varphi_1 d\eta_1 d\varphi_2 d\eta_2\, \mathbb{P}_2(\eta_1,\varphi_1,\eta_2,\varphi_2|m) = 1, \tag{20}$$

as probability densities. The quantities $\langle n\rangle_m$ and $\langle n(n-1)\rangle_m$ are the mean number of particles and the mean number of pairs of particles in the acceptance of the measurement at a given reference multiplicity m; $\mathbb{P}_1(\eta,\varphi|m)$ is the probability of finding a particle at η,φ when the multiplicity is m, and $\mathbb{P}_2(\eta_1,\varphi_1,\eta_2,\varphi_2|m)$ is the joint probability of measuring particles at η_1,φ_1 and η_2,φ_2 when the multiplicity is m. In general, one expects $\langle n\rangle_m$ and $\langle n(n-1)\rangle_m$ to scale approximately linearly and quadratically, respectively, with m. Let us assume that the shape of $\mathbb{P}_1(\eta,\varphi|m)$ and $\mathbb{P}_2(\eta_1,\varphi_1,\eta_2,\varphi_2|m)$ change little through a centrality bin. One can then write

$$R_2^{(\mathrm{Bin},k)}(\eta_1,\varphi_1,\eta_2,\varphi_2) \;=\; \alpha\,\frac{\bar{\mathbb{P}}_2(\eta_1,\varphi_1,\eta_2,\varphi_2)}{\bar{\mathbb{P}}_1(\eta_1,\varphi_1)\bar{\mathbb{P}}_1(\eta_2,\varphi_2)} - 1, \tag{21}$$

with

$$\alpha = \frac{\frac{1}{Q_k}\sum_{m=m_{\mathrm{min},k}}^{m_{\mathrm{max},k}} q(m)\langle n(n-1)\rangle_m}{\left(\frac{1}{Q_k}\sum_{m=m_{\mathrm{min},k}}^{m_{\mathrm{max},k}} q(m)\langle n\rangle_m\right)^2} \tag{22}$$

and $\bar{\mathbb{P}}_1(\eta_1,\varphi_1)$ and $\bar{\mathbb{P}}_2(\eta_1,\varphi_1,\eta_2,\varphi_2)$ are the bin-width averaged values of the single- and two-particle probability densities. Similarly, one can also write

$$\bar{R}_2^{(k)}(\eta_1,\varphi_1,\eta_2,\varphi_2) \;=\; \beta\,\frac{\bar{\mathbb{P}}_2(\eta_1,\varphi_1,\eta_2,\varphi_2)}{\bar{\mathbb{P}}_1(\eta_1,\varphi_1)\bar{\mathbb{P}}_1(\eta_2,\varphi_2)} - 1, \tag{23}$$

with

$$\beta = \frac{1}{Q_k}\sum_{m=m_{\mathrm{min},k}}^{m_{\mathrm{max},k}} q(m)\frac{\langle n(n-1)\rangle_m}{\langle n\rangle_m^2}. \tag{24}$$

One thus finds that for sufficiently narrow bins (such that $\mathbb{P}_1$ and $\mathbb{P}_2$ can be considered approximately invariant within),

$$\bar{R}_2^{(k)}(\eta_1,\varphi_1,\eta_2,\varphi_2) = \beta\alpha^{-1}\left(R_2^{(\mathrm{Bin},k)}(\eta_1,\varphi_1,\eta_2,\varphi_2)+1\right) - 1 \tag{25}$$

The above expression assumes that the event detection efficiency is either unity or constant across a bin k. If the event detection efficiency, $\varepsilon(m)$, varies across $[m_{\mathrm{min},k}, m_{\mathrm{max},k}]$, and the densities $\mathbb{P}_1$ and $\mathbb{P}_2$ are not biased by this dependence, then the coefficients α and β may be written as

$$\alpha \;=\; \frac{\frac{1}{Q_k}\sum_{m=m_{\mathrm{min},k}}^{m_{\mathrm{max},k}} \frac{q^*(m)}{\varepsilon(m)}\langle n(n-1)\rangle_m}{\left(\frac{1}{Q_k}\sum_{m=m_{\mathrm{min},k}}^{m_{\mathrm{max},k}} \frac{q^*(m)}{\varepsilon(m)}\langle n\rangle_m\right)^2}, \tag{26}$$

$$\beta \;=\; \frac{1}{Q_k}\sum_{m=m_{\mathrm{min},k}}^{m_{\mathrm{max},k}} \frac{q^*(m)}{\varepsilon(m)}\frac{\langle n(n-1)\rangle_m}{\langle n\rangle_m^2}, \tag{27}$$

where $q^*(m)$ is now the observed (uncorrected) probability distribution of multiplicity m.

IV. TRANSVERSE MOMENTUM CORRELATORS

Several forms of transverse momentum correlators have been proposed and reported in the recent literature [10, 11, 19–24]. In this work, the focus is on the G_2 correlator proposed by Gavin et al. [11, 20–22] to study transverse momentum current correlations and the P_2 correlator designed to be sensitive to transverse momentum fluctuations [10, 23, 24].

A. G_2 Correlator

At fixed reference multiplicity, m, the differential transverse momentum correlator G_2 can be written as [20]

$$G_2(\eta_1,\varphi_1,\eta_2,\varphi_2|m) = \frac{\int dp_{\rm T,1}\int dp_{\rm T,2}\, p_{\rm T,1}\, p_{\rm T,2}\, \rho_2(\eta_1,\varphi_1,p_{\rm T,1},\eta_2,\varphi_2,p_{\rm T,2}|m)}{\rho_1(\eta_1,\varphi_1|m)\,\rho_1(\eta_2,\varphi_2|m)} - \langle p_{\rm T}(\eta_1,\varphi_1|m)\rangle\langle p_{\rm T}(\eta_2,\varphi_2|m)\rangle \tag{28}$$

where

$$\langle p_{\rm T}(\eta,\varphi|m)\rangle = \frac{\int dp_{\rm T} p_{\rm T}\,\rho_1(\eta,\varphi,p_{\rm T}|m)}{\rho_1(\eta,\varphi|m)} \tag{29}$$

is the event inclusive average particle transverse momentum at η, φ. Evaluation of the centrality-bin averaged $\bar{G}_2^{(k)}(\eta_1,\varphi_1,\eta_2,\varphi_2)$ proceeds as for R_2 and one writes

$$\bar{G}_2^{(k)}(\eta_1,\varphi_1,\eta_2,\varphi_2) = \frac{1}{Q_k}\sum_{m=m_{\min,k}}^{m_{\max,k}} q(m)\, G_2(\eta_1,\varphi_1,\eta_2,\varphi_2|m). \tag{30}$$

Introducing

$$\begin{aligned} S_1(\eta,\varphi|m) &= \int p_{\rm T}\, dp_{\rm T}\,\rho_1(\eta,\varphi,p_{\rm T}|m), &(31)\\ &= \langle n\rangle_m\, \mathbb{P}_1^{p_{\rm T}}(\eta,\varphi|m), &(32)\\ S_2(\eta_1,\varphi_1,\eta_2,\varphi_2|m) &= \int p_{\rm T,1}\, dp_{\rm T,1}\int p_{\rm T,2} dp_{\rm T,2}\,\rho_2(\eta_1,\varphi_1,p_{\rm T,1},\eta_2,\varphi_2,p_{\rm T,2}|m), &(33)\\ &= \langle n(n-1)\rangle_m\, \mathbb{P}_2^{p_{\rm T}p_{\rm T}}(\eta_1,\varphi_1,\eta_2,\varphi_2|m), &(34)\end{aligned}$$

with

$$\begin{aligned} \mathbb{P}_1^{p_{\rm T}}(\eta,\varphi|m) &= \int p_{\rm T}\, dp_{\rm T}\,\mathbb{P}_1(\eta,\varphi,p_{\rm T}|m), &(35)\\ \mathbb{P}_2^{p_{\rm T}p_{\rm T}}(\eta_1,\varphi_1,\eta_2,\varphi_2|m) &= \int p_{\rm T,1}\, dp_{\rm T,1}\int p_{\rm T,2}\, dp_{\rm T,2}\,\mathbb{P}_2(\eta_1,\varphi_1,p_{\rm T,1},\eta_2,\varphi_2,p_{\rm T,2}|m), &(36)\end{aligned}$$

Eq. (28) is written as

$$\begin{aligned} G_2(\eta_1,\varphi_1,\eta_2,\varphi_2|m) &= \frac{S_2(\eta_1,\varphi_1,\eta_2,\varphi_2|m)}{\rho_1(\eta_1,\varphi_1|m)\,\rho_1(\eta_2,\varphi_2|m)} - \frac{S_1(\eta_1,\varphi_1|m)}{\rho_1(\eta_1,\varphi_1|m)}\frac{S_1(\eta_2,\varphi_2|m)}{\rho_1(\eta_2,\varphi_2|m)} &(37)\\ &= \frac{\langle n(n-1)\rangle_m}{\langle n\rangle_m^2}\frac{\mathbb{P}_2^{p_{\rm T}p_{\rm T}}(\eta_1,\varphi_1,\eta_2,\varphi_2|m)}{\mathbb{P}_1(\eta_1,\varphi_1|m)\,\mathbb{P}_1(\eta_2,\varphi_2|m)} - \frac{\mathbb{P}_1^{p_{\rm T}}(\eta_1,\varphi_1|m)}{\mathbb{P}_1(\eta_1,\varphi_1|m)}\frac{\mathbb{P}_1^{p_{\rm T}}(\eta_2,\varphi_2|m)}{\mathbb{P}_1(\eta_2,\varphi_2|m)}. &(38)\end{aligned}$$

If the ratios $\mathbb{P}_1^{p_{\rm T}}/\mathbb{P}_1$ and $\mathbb{P}_2^{p_{\rm T}p_{\rm T}}/\mathbb{P}_1\mathbb{P}_1$ have a modest dependence on the reference multiplicity (within a bin k), then it is legitimate to replace them by averages and one gets

$$G_2(\eta_1,\varphi_1,\eta_2,\varphi_2|m) = \frac{\langle n(n-1)\rangle_m}{\langle n\rangle_m^2}\frac{\bar{\mathbb{P}}_2^{p_{\rm T}p_{\rm T}(k)}(\eta_1,\varphi_1,\eta_2,\varphi_2)}{\bar{\mathbb{P}}_1^{(k)}(\eta_1,\varphi_1)\,\bar{\mathbb{P}}_1^{(k)}(\eta_2,\varphi_2)} - \frac{\bar{\mathbb{P}}_1^{p_{\rm T}(k)}(\eta_1,\varphi_1)}{\bar{\mathbb{P}}_1^{(k)}(\eta_1,\varphi_1)}\frac{\bar{\mathbb{P}}_1^{p_{\rm T}(k)}(\eta_2,\varphi_2)}{\bar{\mathbb{P}}_1^{(k)}(\eta_2,\varphi_2)}. \tag{39}$$

The centrality-bin averaged correlator $\bar{G}_2^{(k)}(\eta_1,\varphi_1,\eta_2,\varphi_2)$ may then be written as

$$\bar{G}_2^{(k)}(\eta_1,\varphi_1,\eta_2,\varphi_2) = \beta\frac{\bar{\mathbb{P}}_2^{p_{\rm T}p_{\rm T}(k)}(\eta_1,\varphi_1,\eta_2,\varphi_2)}{\bar{\mathbb{P}}_1^{(k)}(\eta_1,\varphi_1)\,\bar{\mathbb{P}}_1^{(k)}(\eta_2,\varphi_2)} - \frac{\bar{\mathbb{P}}_1^{p_{\rm T}(k)}(\eta_1,\varphi_1)}{\bar{\mathbb{P}}_1^{(k)}(\eta_1,\varphi_1)}\frac{\bar{\mathbb{P}}_1^{p_{\rm T}(k)}(\eta_2,\varphi_2)}{\bar{\mathbb{P}}_1^{(k)}(\eta_2,\varphi_2)}, \tag{40}$$

with β defined as in (24). However, if it is not possible to carry out the analysis in fine (unit) bins of m, the numerators and denominators of G_2 must be separately averaged over the range $[m_{\min,k}, m_{\max,k}]$. Assuming the ratios $\mathbb{P}_1^{p_\mathrm{T}}/\mathbb{P}_1$ and $\mathbb{P}_2^{p_\mathrm{T}p_\mathrm{T}}/\mathbb{P}_1\mathbb{P}_1$ have a modest dependence on the reference multiplicity, one gets

$$G_2^{(\mathrm{Bin},k)}(\eta_1,\varphi_1,\eta_2,\varphi_2) = \alpha\frac{\bar{\mathbb{P}}_2^{p_\mathrm{T}p_\mathrm{T}(k)}(\eta_1,\varphi_1,\eta_2,\varphi_2)}{\bar{\mathbb{P}}_1^{(k)}(\eta_1,\varphi_1)\,\bar{\mathbb{P}}_1^{(k)}(\eta_2,\varphi_2)} - \frac{\bar{\mathbb{P}}_1^{p_\mathrm{T}(k)}(\eta_1,\varphi_1)}{\bar{\mathbb{P}}_1^{(k)}(\eta_1,\varphi_1)}\frac{\bar{\mathbb{P}}_1^{p_\mathrm{T}(k)}(\eta_2,\varphi_2)}{\bar{\mathbb{P}}_1^{(k)}(\eta_2,\varphi_2)}, \tag{41}$$

with α defined as in (22). Identifying $\langle p_\mathrm{T}(\eta,\varphi)\rangle^{(\mathrm{Bin},k)} = \bar{\mathbb{P}}_1^{p_\mathrm{T}(k)}(\eta,\varphi)/\bar{\mathbb{P}}_1^{(k)}(\eta,\varphi)$, one finally gets that the desired correlator $\bar{G}_2^{(k)}(\eta_1,\varphi_1,\eta_2,\varphi_2)$ may be determined as

$$\begin{aligned}\bar{G}_2^{(k)}(\eta_1,\varphi_1,\eta_2,\varphi_2) =& \beta\alpha^{-1}\left(G_2^{(\mathrm{Bin},k)}(\eta_1,\varphi_1,\eta_2,\varphi_2) + \langle p_\mathrm{T}(\eta_1,\varphi_1)\rangle^{(\mathrm{Bin},k)}\langle p_\mathrm{T}(\eta_2,\varphi_2)\rangle^{(\mathrm{Bin},k)}\right)\\ &- \langle p_\mathrm{T}(\eta_1,\varphi_1)\rangle^{(\mathrm{Bin},k)}\langle p_\mathrm{T}(\eta_2,\varphi_2)\rangle^{(\mathrm{Bin},k)},\\ =& \beta\alpha^{-1}G_2^{(\mathrm{Bin},k)}(\eta_1,\varphi_1,\eta_2,\varphi_2) + \left(\beta\alpha^{-1}-1\right)\langle p_\mathrm{T}(\eta_1,\varphi_1)\rangle^{(\mathrm{Bin},k)}\langle p_\mathrm{T}(\eta_2,\varphi_2)\rangle^{(\mathrm{Bin},k)}.\end{aligned} \tag{42}$$

B. P_2 Correlator

The P_2 correlator is defined as

$$P_2(\eta_1,\varphi_1,\eta_2,\varphi_2|m) \;=\; \frac{1}{\langle p_\mathrm{T}\rangle^2}\frac{\int\Delta p_{\mathrm{T},1}dp_{\mathrm{T},1}\int\Delta p_{\mathrm{T},2}dp_{\mathrm{T},2}\,\rho_2(\eta_1,\varphi_1,p_{\mathrm{T},1},\eta_2,\varphi_2,p_{\mathrm{T},2}|m)}{\rho_2(\eta_1,\varphi_1,\eta_2,\varphi_2|m)}, \tag{43}$$

where $\Delta p_{\mathrm{T,i}} \equiv p_{\mathrm{T,i}} - \langle p_\mathrm{T}\rangle$ and the $\langle p_\mathrm{T}\rangle^2$ normalization insures P_2 is dimensionless. Introducing (44) one next verifies that P_2 is insensitive to multiplicity fluctuations [10, 23, 24].

$$\mathbb{P}_2^{\Delta p_\mathrm{T}\Delta p_\mathrm{T}}(\eta_1,\varphi_1,\eta_2,\varphi_2|m) \;=\; \int\Delta p_{\mathrm{T},1}dp_{\mathrm{T},1}\int\Delta p_{\mathrm{T},2}dp_{\mathrm{T},2}\,\mathbb{P}_2(\eta_1,\varphi_1,p_{\mathrm{T},1},\eta_2,\varphi_2,p_{\mathrm{T},2}|m) \tag{44}$$

Factorizing the two-particle density as in (18), one gets

$$P_2(\eta_1,\varphi_1,\eta_2,\varphi_2|m) \;=\; \left(\frac{\mathbb{P}_1}{\mathbb{P}_1^{p_\mathrm{T}}}\right)^2\frac{\langle n(n-1)\rangle_m}{\langle n(n-1)\rangle_m}\frac{\mathbb{P}_2^{\Delta p_\mathrm{T}\Delta p_\mathrm{T}}(\eta_1,\varphi_1,\eta_2,\varphi_2|m)}{\mathbb{P}_2(\eta_1,\varphi_1,\eta_2,\varphi_2|m)}. \tag{45}$$

If the ratios $\mathbb{P}_1^{p_\mathrm{T}}/\mathbb{P}_1$ and $\mathbb{P}_2^{\Delta p_\mathrm{T}\Delta p_\mathrm{T}}/\mathbb{P}_2$ have a modest dependence on the reference multiplicity (within a bin k), then it is legitimate to replace them by averages and one gets

$$P_2(\eta_1,\varphi_1,\eta_2,\varphi_2|m) \;=\; \left(\frac{\bar{\mathbb{P}}_1^{(k)}}{\bar{\mathbb{P}}_1^{p_\mathrm{T}(k)}}\right)^2\frac{\bar{\mathbb{P}}_2^{\Delta p_\mathrm{T}\Delta p_\mathrm{T}(k)}(\eta_1,\varphi_1,\eta_2,\varphi_2)}{\bar{\mathbb{P}}_2^{(k)}(\eta_1,\varphi_1,\eta_2,\varphi_2)}, \tag{46}$$

which is indeed independent of the number of pairs and thus multiplicity fluctuations, since the functions $\bar{\mathbb{P}}_2(\eta_1,\varphi_1,\eta_2,\varphi_2|m)$ are probability densities. The centrality-bin averaged value of P_2 is calculated according

$$\bar{P}_2^{(k)}(\eta_1,\varphi_1,\eta_2,\varphi_2) \;=\; \left(\frac{\bar{\mathbb{P}}_1^{(k)}}{\bar{\mathbb{P}}_1^{p_\mathrm{T}(k)}}\right)^2\frac{\bar{\mathbb{P}}_2^{\Delta p_\mathrm{T}\Delta p_\mathrm{T}(k)}(\eta_1,\varphi_1,\eta_2,\varphi_2)}{\bar{\mathbb{P}}_2^{(k)}(\eta_1,\varphi_1,\eta_2,\varphi_2)}, \tag{47}$$

while the ratio of bin averages is

$$P_2^{(\mathrm{Bin},k)}(\eta_1,\varphi_1,\eta_2,\varphi_2) \;=\; \left(\frac{\bar{\mathbb{P}}_1^{(k)}}{\bar{\mathbb{P}}_1^{p_\mathrm{T}(k)}}\right)^2\frac{\bar{\mathbb{P}}_2^{\Delta p_\mathrm{T}\Delta p_\mathrm{T}(k)}(\eta_1,\varphi_1,\eta_2,\varphi_2)}{\bar{\mathbb{P}}_2^{(k)}(\eta_1,\varphi_1,\eta_2,\varphi_2)}. \tag{48}$$

One thus finds that

$$\bar{P}_2^{(k)}(\eta_1,\varphi_1,\eta_2,\varphi_2) \;=\; P_2^{(\mathrm{Bin},k)}(\eta_1,\varphi_1,\eta_2,\varphi_2), \tag{49}$$

featuring a unitary correction factor. The P_2 correlator is thus indeed not affected by the width of the multiplicity bins so long as the probability densities $\mathbb{P}_1$ and $\mathbb{P}_2$ exhibit only modest shape variations within those bins.

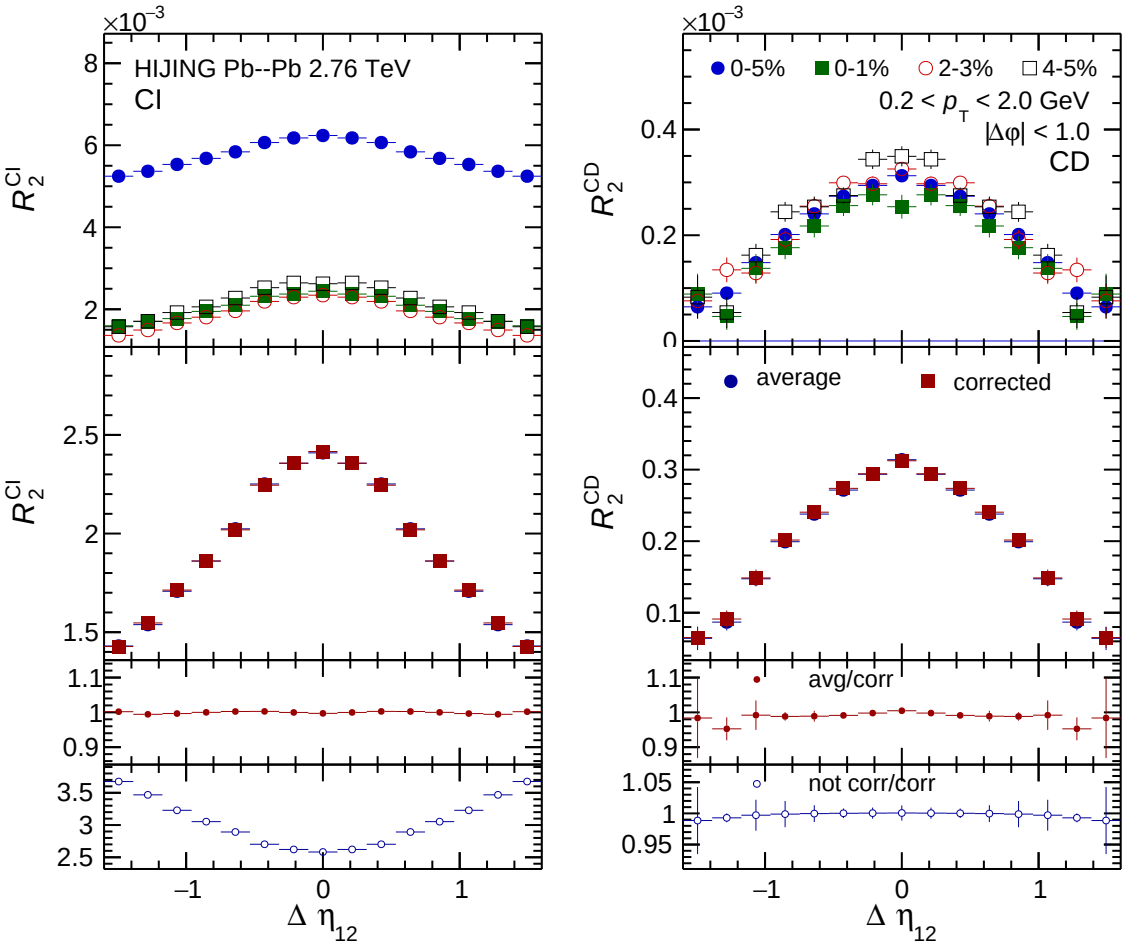

FIG. 1. Longitudinal projection of the two-particle normalized cumulants $R_2^{\rm CI}$ (left) and $R_2^{\rm CD}$ (right) for the most central Pb–Pb collisions produced with the HIJING event generator. Top panels show uncorrected results for the 0-5% centrality bin together with those from the 0-1%, 2-3%, and 4-5% centrality bins, middle panels show corrected 0-5% centrality bin results compared with the weighted average of those from the 0-1%, 1-2%, 2-3%, 3-4% and 4-5% centrality bins, while bottom panels show their ratio.

V. SIMULATIONS

The accuracy of the centrality bin width correction methods defined by Eqs. (25) and (42) is tested using HIJING and UrQMD simulations of 5% most central central Pb–Pb collisions at $\sqrt{s_{\rm NN}} = 2.76$ TeV. Overall, 65,000 and 100,000 Pb–Pb collisions from HIJING and UrQMD were used for this study. The collision centrality classification used for HIJING events mimics the method used by the ALICE collaboration [25, 26] and is based on the number of charged particles in the pseudo-rapidity ranges $2.8 < \eta < 5.1$ and $-3.7 < \eta < -1.7$ corresponding to the acceptance of the ALICE V0 detectors. For UrQMD simulations, the centrality selection is based on sharp cuts in the impact parameter of the collision, as given in [25]. The impact of the centrality estimation method is not considered in this work. It is assumed that the centrality is properly extracted and that the method employed to estimate it does not influence the results. In actual measurements, the impact of the centrality estimation method shall be inferred with the usual methods for systematic uncertainties extraction. The R_2, G_2, and P_2 correlators for charged particle combinations ($+-$, $-+$, $--$ and $++$) are first determined as 4-dimensional functions based on generator level charged hadrons in the ranges $0.2 \leq p_{\rm T} \leq 2.0$ GeV/c and $|\eta| < 0.8$ using Eqs. (25), (42), and (49). From these, the charge independent CI and charge dependent CD particle combinations are calculated according to

$$C^{\rm CI} = \frac{1}{4}\left[C^{(+-)} + C^{(-+)} + C^{(--)} + C^{(++)}\right] \tag{50}$$

$$C^{\rm CD} = \frac{1}{4}\left[C^{(+-)} + C^{(-+)} - C^{(--)} - C^{(++)}\right]. \tag{51}$$

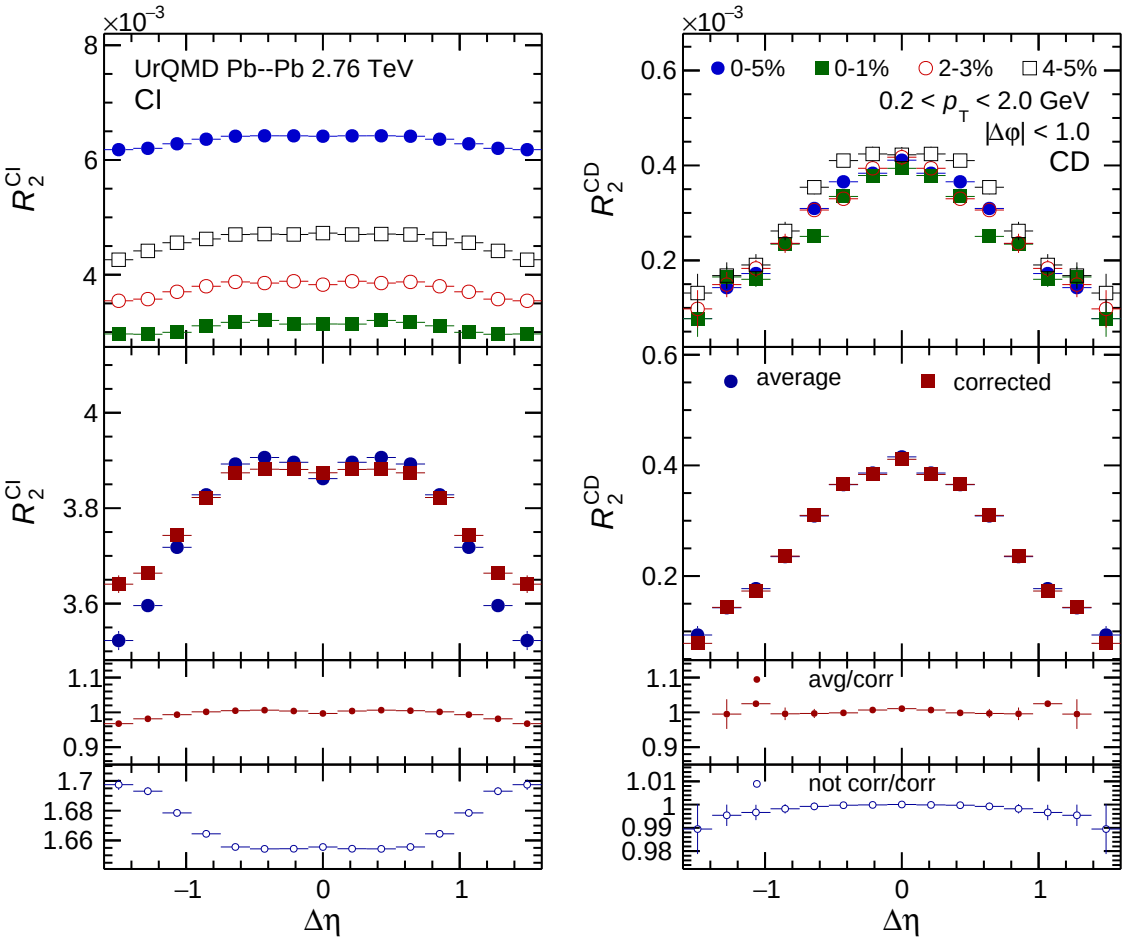

FIG. 2. Longitudinal projection of the two-particle normalized cumulants $R_2^{\rm CI}$ (left) and $R_2^{\rm CD}$ (right) for 5% most central Pb–Pb collisions produced with the UrQMD event generator. Top panels show uncorrected results for the 0-5% centrality bin together with those from the 0-1%, 2-3%, and 4-5% centrality bins, middle panels show corrected 0-5% centrality bin results compared with the weighted average of those from the 0-1%, 1-2%, 2-3%, 3-4% and 4-5% centrality bins, while bottom panels show their ratio.

where C stands for any of the R_2, G_2, and P_2 correlators. Projections of these correlators onto $\Delta\eta$ and $\Delta\varphi$ were computed using the integer arithmetic technique described in [12].

Figure 1 presents $\Delta\eta$ projections of the $R_2^{\rm CI}$ (left) and $R_2^{\rm CD}$ (right) correlation functions based on 5% most central HIJING events. The top panels of the figure present uncorrected results for 0-5% (blue), 0-1% (green), 2-3% (red), and 4-5% (black). The bottom panels displays 0-5% centrality results corrected with Eq. (25) (blue) compared to the weighted mean of the correlators obtained for 0-1%, 1-2%, 2-3%, 3-4%, and 4-5% centralities (red) and their ratio. One finds that the results corrected with Eq. (25) agree with those obtained with the weighted mean within 1% for both $R_2^{\rm CI}$ and $R_2^{\rm CD}$.

Similar results are presented in Fig. 2 for the UrQMD model. In this case, agreement between the 0-5% corrected R_2 correlators and the weighted mean of the R_2 correlators obtained in 0-1%, 1-2%, 2-3%, 3-4%, and 4-5% centralities is found to be also within 1% for both $R_2^{\rm CI}$ and $R_2^{\rm CD}$. Thus, based on the HIJING and UrQMD model simulations presented, it is concluded that Eq. (25) enables reasonably accurate corrections of the R_2 correlators in the context of these two models. Given these models provide relatively realistic representations of single and pair particle spectra, the correction method embodied in Eq. (25) should provide reasonably reliable bin-width corrections of R_2 correlation functions measured at any heavy ion collider.

Figures 3 and 4 present $\Delta\eta$ projections of the $G_2^{\rm CI}$ and $G_2^{\rm CD}$ correlation functions based on 5% most central events from HIJING and UrQMD models respectively. Similarly as in previous figures, the top panels display uncorrected G_2 correlators for 0-5% (blue), 0-1% (green), 2-3% (red), and 4-5% (black) while the bottom panels display 0-5% centrality results corrected with Eq. (42) (blue) compared to the weighted mean of the G_2 correlators obtained for 0-1%, 1-2%, 2-3%, 3-4%, and 4-5% centralities (red) and their ratio. Comparing the corrected results with the weighted

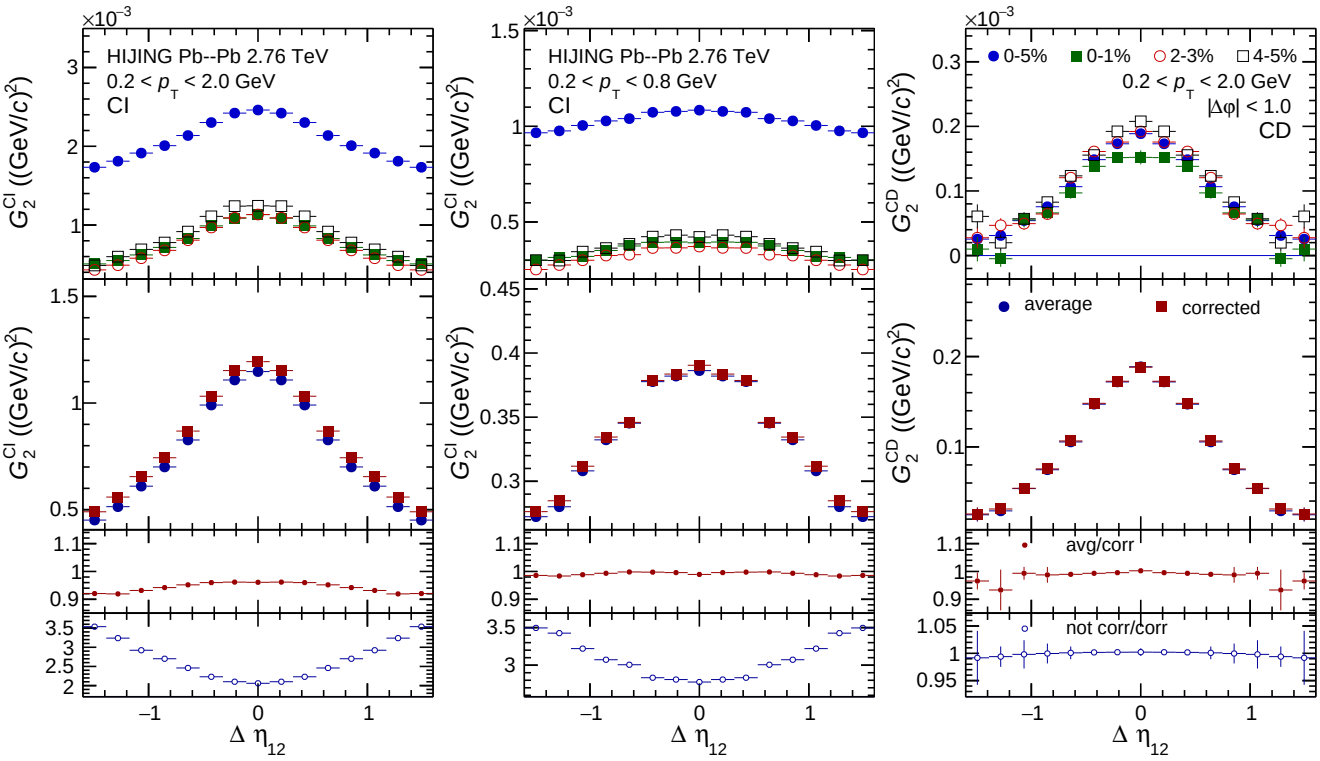

FIG. 3. Longitudinal projection of the two-particle transverse momentum correlations $G_2^{\rm CI}$ for default transverse momentum range particles (left) and for the reduced (see text) transverse momentum range particles (center) and $G_2^{\rm CD}$ for the default transverse momentum range particles (right) for the 5% most central Pb–Pb collisions produced with the HIJING event generator. Top panels show uncorrected results for the 0-5% centrality bin together with those from the 0-1%, 1-2%, 2-3%, 3-4% and 4-5% centrality bins, middle panels show corrected 0-5% centrality bin results compared with the weighted average of those from the 0-1%, 1-2%, 2-3%, 3-4% and 4-5% centrality bins, while bottom panels show their ratio.

averages for HIJING events one finds them within 7% for $G_2^{\rm CI}$ and within 1% for $G_2^{\rm CD}$ while the comparison for UrQMD events leaves them within 1% for both $G_2^{\rm CI}$ and $G_2^{\rm CD}$.

The discrepancy between the correction level achieved for $G_2^{\rm CI}$ for collisions simulated with HIJING compared with those produced using UrQMD is hardly satisfactory, especially considering the 1% correction precision achieved, with both models, for the $R_2^{\rm CI}$ correlator. Given the transverse momentum enters explicitly into the expression of the G_2 correlator, but not in R_2, to determine whether the $p_{\rm T}$ range considered may influence the correction precision achievable with Eq. (42) the above study is repeated for charged particles in the range 0.2-0.8 GeV/c. Central panels of Fig. 3 display $\Delta\eta$ projections of the $G_2^{\rm CI}$ correlation function based on 5% most central events from HIJING model for particle within the transverse momentum range 0.2-0.8 GeV/c. As before, the top panel shows a comparison of the correlators calculated within the 0-5% centrality bin with those from the 0-1%, 2-3% and 4-5% centrality bins, while the bottom panel displays 0-5% centrality results corrected with Eq. (42) compared to the weighted mean of the values obtained in the 0-1%, 1-2%, 2-3%, 3-4%, and 4-5% collision centrality bins. It is found that the 0-5% centrality corrected result is now within 1% of the weighted mean of those obtained with finer centrality bins. The centrality dependence of the single- and two-particle probability densities (and their $p_{\rm T}$ weighted counterparts, Eqs. (35) and (36)) is then examined, and found that those obtained within the 0.2-0.8 GeV/c range feature a quantitatively smaller dependence of collision centrality than those integrated in the 0.2-2.0 GeV/c range. The former range consequently better satisfies the condition, implicit in Eq. (41), that the densities be approximately independent of collision centrality, within each centrality bin k. That these densities, calculated within the range 0.2-2.0 GeV/c with UrQMD events, similarly exhibit very little shape dependence on collision centrality is additionally verified. This analysis confirms the relevance of the proper behavior of this magnitudes established in section IV A. As conclusion then, the finite centrality bin width correction, included in Eq. (42), under the criteria established for its deduction, provides a reasonably accurate correction technique for G_2 correlators to account for collision centrality average when using finite collision centrality bins.

It is worth highlighting that, consistently with what was naively expected, the centrality bin width effect is completely charge independent. Indeed, the amplitude of both $R_2^{\rm CI}$ and $G_2^{\rm CI}$ are substantially affected by the wide

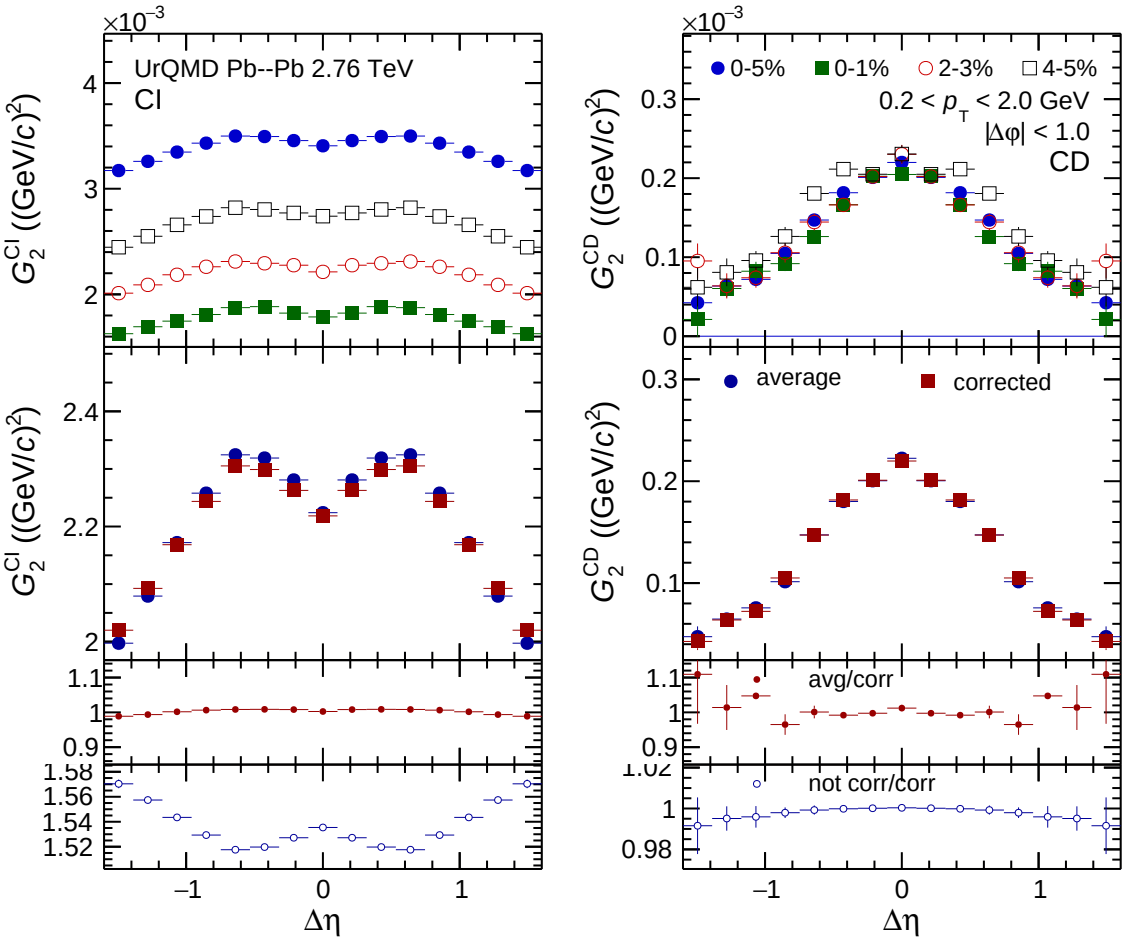

FIG. 4. Longitudinal projection of the two-particle transverse momentum correlations $G_2^{\rm CI}$ (left) and $G_2^{\rm CD}$ (right) for the 5% most central Pb–Pb collisions produced with the UrQMD event generator. Top panels show uncorrected results for the 0-5% centrality bin together with those from the 0-1%, 1-2%, 2-3%, 3-4% and 4-5% centrality bins, middle panels show corrected 0-5% centrality bin results compared with the weighted average of those from the 0-1%, 1-2%, 2-3%, 3-4% and 4-5% centrality bins, while bottom panels show their ratio.

centrality bin averaging while $R_2^{\rm CD}$ and $G_2^{\rm CD}$ only experience a minor shift owing (1) to the very small differences between the $R_2^{\rm LS}$ and $R_2^{\rm US}$ correlator dependence on particle densities and on the transverse momentum of the particles, and (2) to the approximately equal number of US and LS pairs observed at large $\sqrt{s_{\rm NN}}$ in the central rapidity range.

For the sake of completeness, the behavior of the correction procedures on the $\Delta\varphi$ projections of $R_2^{\rm CI}$ (for the whole $p_{\rm T}$ range) and $G_2^{\rm CI}$ (for the reduced $p_{\rm T}$ range) correlators are shown in Fig. 5. The correction procedures yield essentially perfect corrections of these $\Delta\varphi$ projections for both correlators. Additionally, the applicability of Eq. (49) for $P_2^{\rm CI}$ correlators is demonstrated in Fig. 6 where it is shown that the $P_2^{\rm CI}$ correlator determined with a 0-5% centrality bin is virtually identical to that obtained with a weighted average of the correlators calculated from the 0-1%, 1-2%, 2-3%, 3-4%, and 4-5% collision centrality bins.

Finally, in order to obtain a quantitative assessment of the precision of the centrality bin width correction procedures embodied by Eqs. (25,49,42), the ratios of the centrality bin width corrected correlators to those obtained with weighted averages of correlators obtained in fine width centrality bins, shown in Figs. 1-6, are fitted with a constant polynomial (POL0 in ROOT [27]). Fitted values of the ratios, corresponding to ratios averaged across the $\Delta\eta$ and $\Delta\varphi$ fiducial ranges, are listed in Table I.

Overall, it is found that the averaged ratios have values consistent with unity within statistical errors (i.e., within a $\pm 2\sigma$, 96% confidence interval), thereby implying that within the statistical precision achieved in this work, it can be concluded that the correction procedures do not introduce a significant bias to the correlation functions. Notable exceptions are the values obtained with both $\Delta\eta$ and $\Delta\phi$ projections for $G_2^{\rm CI}$ when this correlator is calculated for charged particles in the range $0.2 \leq p_{\rm T} \leq 2.0$ GeV/c with HIJING. However, the ratios of these projections are consistent with unity when the correlator is calculated in a narrower $p_{\rm T}$ range in line with the demanded behavior of

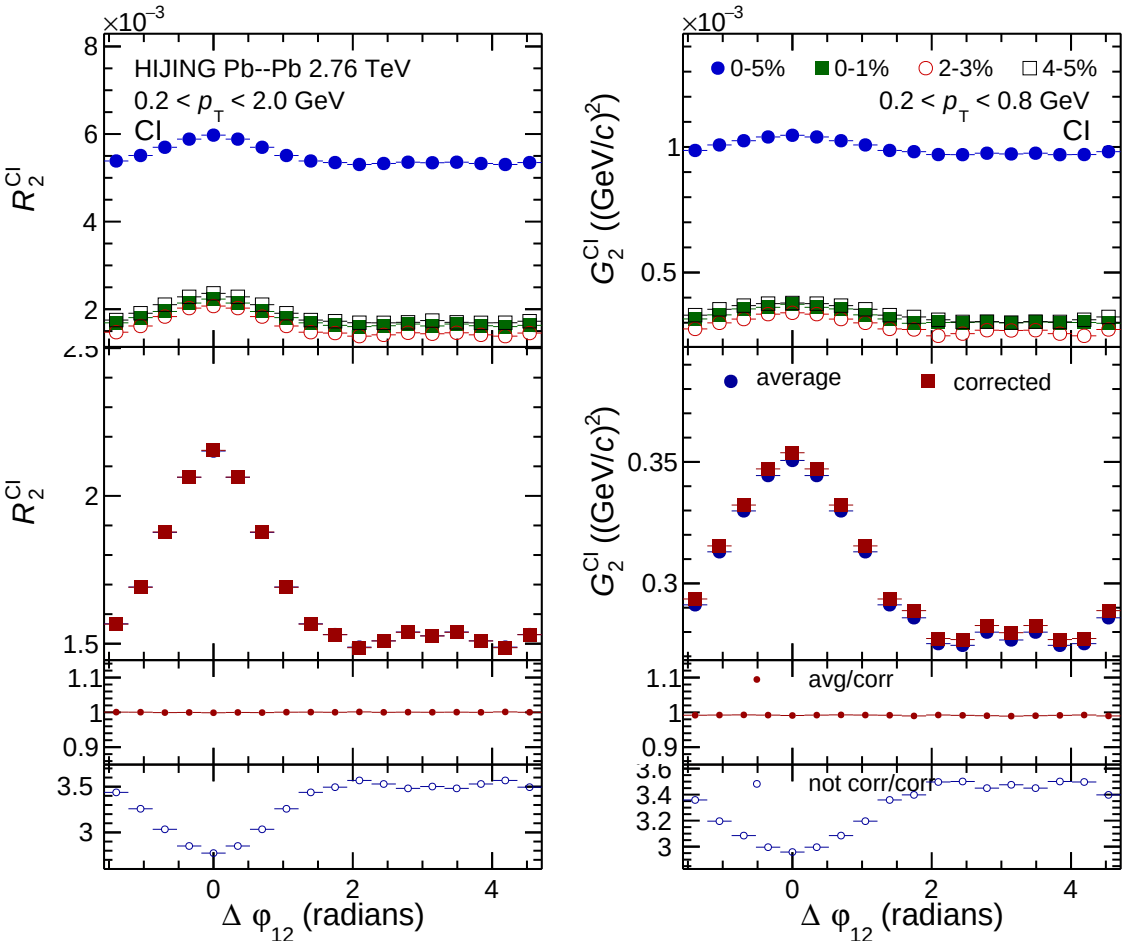

FIG. 5. Azimuthal projections of the two-particle transverse momentum correlations $R_2^{\rm CI}$ for the whole $p_{\rm T}$ range (left) and $G_2^{\rm CI}$ for the reduced $p_{\rm T}$ range (right) for the 5% most central Pb–Pb collisions produced with the HIJING event generator. Top panels show uncorrected results for the 0-5% centrality bin together with those from the 0-1%, 1-2%, 2-3%, 3-4% and 4-5% centrality bins, middle panels show corrected 0-5% centrality bin results compared with the weighted average of those from the 0-1%, 1-2%, 2-3%, 3-4% and 4-5% centrality bins, while bottom panels show their ratio.

TABLE I. *POL0* fit to the ratio 0-5% centrality corrected versus 0-1%, 1-2%, 2-3%, 3-4%, and 4-5% centralities weighted mean.

Model	proj.	$R_2^{\rm CI}$	$R_2^{\rm CD}$	$P_2^{\rm CI}$	$P_2^{\rm CD}$	$G_2^{\rm CI}$	$G_2^{\rm CD}$
HIJING	$\Delta\eta$	1.000 ± 0.001	0.995 ± 0.003	0.989 ± 0.002	0.999 ± 0.004	0.931 ± 0.001	0.997 ± 0.002
HIJING	$\Delta\varphi$	1.000 ± 0.001	0.988 ± 0.003	0.987 ± 0.003	0.994 ± 0.008	0.935 ± 0.001	0.985 ± 0.004
UrQMD	$\Delta\eta$	1.001 ± 0.0003	1.005 ± 0.0016	1.010 ± 0.0012	0.893 ± 0.0435	1.007 ± 0.001	1.002 ± 0.002
UrQMD	$\Delta\varphi$	0.990 ± 0.0002	1.047 ± 0.0027	1.022 ± 0.0007	1.040 ± 0.0222	1.008 ± 0.001	0.985 ± 0.003
HIJING low $p_{\rm T}$	$\Delta\eta$					0.995 ± 0.001	0.993 ± 0.006
HIJING low $p_{\rm T}$	$\Delta\varphi$					0.991 ± 0.001	0.989 ± 0.002

the probability density distributions. A large discrepancy is also seemingly observed for the $P_2^{\rm CD}$ correlator obtained with the UrQMD simulation. However, the overall magnitude of $P_2^{\rm CD}$ predicted by UrQMD is a seventh of that obtained with HIJING events and correlation amplitudes are nearly vanishing, within statistical accuracy, across a wide $\Delta\eta_{12}$ range. A proper evaluation of the correction is thus more challenging in this case.

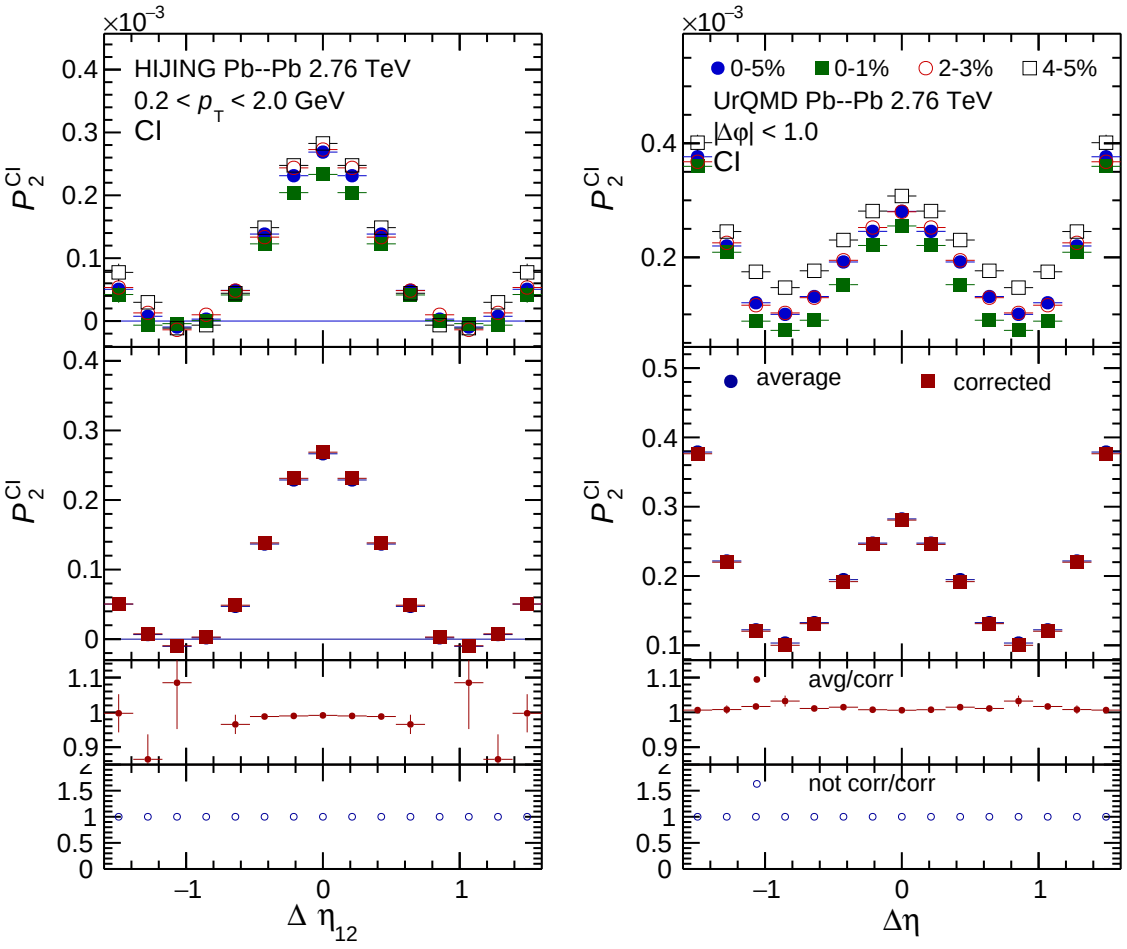

FIG. 6. Longitudinal projection of the two-particle transverse momentum correlation P_2^{CI} for the 5% most central Pb–Pb collisions produced with the HIJING event generator (left) and the UrQMD event generator (right). Top panels show uncorrected results for the 0-5% centrality bin together with those from the 0-1%, 1-2%, 2-3%, 3-4% and 4-5% centrality bins, middle panels show corrected 0-5% centrality bin results compared with the weighted average of those from the 0-1%, 1-2%, 2-3%, 3-4% and 4-5% centrality bins, while bottom panels show their ratio.

VI. SUMMARY

Studies of the centrality or particle multiplicity evolution of the integral and amplitudes of two-particle number and transverse momentum differential correlations, as tools to gain insights into particle production and transport dynamics in heavy-ion collisions, are a growing research field of interest, as recent analyses from the ALICE collaboration show [23, 24]. The bias introduced on the amplitudes and integrals of R_2, G_2 and P_2 correlators when measured directly in wide collision centrality bins, was shown. Correction techniques to be applied to those correlators, when the need for them to be measured on such centrality bins is in place, were described. These correction techniques were tested with HIJING and UrQMD simulations of Pb–Pb collisions at $\sqrt{s_{\mathrm{NN}}} = 2.76$ TeV. They enable a precision of the order of 1%, or better, when using 5% wide centrality bins. Clearly, the reached precision has a direct impact on both the amplitude and the integral of the correlation functions which will allow a better description or constrain of the underlying physics.

ACKNOWLEDGEMENTS

The authors thank the ALICE collaboration for access to a sample of simulated HIJING events used in this analysis and the GSI Helmholtzzentrum für Schwerionenforschung for providing the computational resources needed for producing the UrQMD events used in this analysis. This work was supported in part by the United States

Department of Energy, Office of Nuclear Physics (DOE NP), United States of America under Award Number DE-FG02-92ER-40713 and by Consejo Nacional de Ciencia y Tecnologia (CONACYT), through Fondo de Cooperacion Internacional en Ciencia y Tecnologia (FONCICYT) and Direccion General de Asuntos del Personal Academico (DGAPA), Mexico.

[1] J. Adams *et al.* (STAR), Nucl. Phys. **A757**, 102 (2005), arXiv:nucl-ex/0501009 [nucl-ex].
[2] K. Adcox *et al.* (PHENIX), Nucl. Phys. **A757**, 184 (2005), arXiv:nucl-ex/0410003 [nucl-ex].
[3] I. Arsene *et al.* (BRAHMS), Nucl. Phys. **A757**, 1 (2005), arXiv:nucl-ex/0410020 [nucl-ex].
[4] B. B. Back *et al.*, Nucl. Phys. **A757**, 28 (2005), arXiv:nucl-ex/0410022 [nucl-ex].
[5] K. Aamodt *et al.* (ALICE), Phys. Rev. Lett. **105**, 252301 (2010), arXiv:1011.3916 [nucl-ex].
[6] K. Aamodt *et al.* (ALICE), Phys. Rev. Lett. **105**, 252302 (2010), arXiv:1011.3914 [nucl-ex].
[7] G. Aad *et al.* (ATLAS Collaboration), Phys. Rev. Lett. **105**, 252303 (2010).
[8] J. Adam *et al.* (ALICE), Phys. Rev. Lett. **116**, 222302 (2016), arXiv:1512.06104 [nucl-ex].
[9] J. Adam *et al.* (ALICE), Phys. Rev. Lett. **116**, 132302 (2016), arXiv:1602.01119 [nucl-ex].
[10] M. Sharma and C. A. Pruneau, Phys. Rev. **C79**, 024905 (2009), arXiv:0810.0716 [nucl-ex].
[11] H. Agakishiev *et al.* (STAR), Phys. Lett. **B704**, 467 (2011), arXiv:1106.4334 [nucl-ex].
[12] S. Ravan, P. Pujahari, S. Prasad, and C. A. Pruneau, Phys. Rev. C **89**, 024906 (2014).
[13] J. Adams *et al.* (STAR), Phys. Rev. **C72**, 044902 (2005), arXiv:nucl-ex/0504031 [nucl-ex].
[14] B. B. Abelev *et al.* (ALICE), Eur. Phys. J. **C74**, 3077 (2014), arXiv:1407.5530 [nucl-ex].
[15] X.-N. Wang and M. Gyulassy, Phys. Rev. D **44**, 3501 (1991).
[16] S. A. Bass *et al.*, Prog. Part. Nucl. Phys. **41**, 255 (1998), [Prog. Part. Nucl. Phys.41,225(1998)], arXiv:nucl-th/9803035 [nucl-th].
[17] M. Bleicher *et al.*, J. Phys. **G25**, 1859 (1999), arXiv:hep-ph/9909407 [hep-ph].
[18] R. Rogly, G. Giacalone, and J.-Y. Ollitrault, (2018), arXiv:1804.03031 [nucl-th].
[19] J. Adams *et al.* (STAR), J. Phys. **G32**, L37 (2006), arXiv:nucl-ex/0509030 [nucl-ex].
[20] M. Abdel-Aziz and S. Gavin, Acta Phys. Hung. **A25**, 515 (2006).
[21] S. Gavin, G. Moschelli, and C. Zin, *Proceedings, 32th Winter Workshop on Nuclear Dynamics (WWND 2016): Guadeloupe, French West Indies*, J. Phys. Conf. Ser. **736**, 012020 (2016), arXiv:1608.05389 [nucl-th].
[22] S. Gavin, G. Moschelli, and C. Zin, Phys. Rev. **C94**, 024921 (2016), arXiv:1606.02692 [nucl-th].
[23] S. Acharya *et al.* (ALICE Collaboration), Phys. Rev. Lett. **118**, 162302 (2017), arXiv:1702.02665 [nucl-ex].
[24] S. Acharya *et al.* (ALICE), (2018), arXiv:1805.04422 [nucl-ex].
[25] B. Abelev *et al.* (ALICE), Phys. Rev. **C88**, 044909 (2013), arXiv:1301.4361 [nucl-ex].
[26] B. B. Abelev *et al.* (ALICE), Int. J. Mod. Phys. **A29**, 1430044 (2014), arXiv:1402.4476 [nucl-ex].
[27] R. Brun and F. Rademakers, *New computing techniques in physics research V. Proceedings, 5th International Workshop, AIHENP '96, Lausanne, Switzerland, September 2-6, 1996*, Nucl. Instrum. Meth. **A389**, 81 (1997).